water

MDPI

Article

Hydraulic Planning in Insular Urban Territories: The Case of Madeira Island—Ribeira Brava, Tabua

Sérgio Lousada [1,2,3,4,5,*], Raul Alves [6], Mário Fernandes [1,7] and Leonardo Gonçalves [1]

1 Department of Civil Engineering and Geology (DECG), Faculty of Exact Sciences and Engineering (FCEE), University of Madeira (UMa), 9000-082 Funchal, Madeira, Portugal; ptsmario2001@gmail.com (M.F.); leonardobazilio13@gmail.com (L.G.)
2 CITUR—Madeira—Research Centre for Tourism Development and Innovation, 9000-082 Funchal, Madeira, Portugal
3 VALORIZA—Research Centre for Endogenous Resource Valorization, Polytechnic Institute of Portalegre (IPP), 9000-082 Portalegre, Portugal
4 Research Group on Environment and Spatial Planning (MAOT), University of Extremadura, 06071 Badajoz, Spain
5 RISCO—Civil Engineering Department, University of Aveiro, 3810-193 Aveiro, Portugal
6 Machico City Council (CMM), Largo do Município Machico, 9200-099 Machico, Portugal; raul@cm-machico.pt
7 Faculty of Economics, University of Porto (FEP), 4200-464 Porto, Portugal
* Correspondence: slousada@staff.uma.pt; Tel.: +351-963-611-712

Abstract: This study's primary goal was to conduct an analysis of the flood propensity of the Tabua (Ribeira Brava) drainage basin's main watercourse. In addition to that, this study also recommends two different methodologies in order to mitigate flood impacts, namely by dimensioning a detention basin and adjusting the riverbed roughness coefficient. Regarding the study on the flood propensity, it was necessary to resort to geomorphological data, which were obtained when characterizing the watershed; these data were crucial to determining the expected peak flow rate, according to the Gumbel distribution methodology and considering a 100-year return period, and to perform necessary tasks in the SIG ArcGIS 10.5 software. Lastly, the drainage capacity of this drainage basin's river mouth was also analyzed in order to conclude whether it would have the capacity to drain the total volume of rainwater if an extreme flood event were to happen. Indeed, the main results show that this watershed's river mouth does not have the necessary drainage capacity to cope with an extreme event for the return period that was considered. As a consequence, the two aforementioned mitigation measures were developed considering the Tabua (Ribeira Brava) drainage basin's specific features. The size of the detention basin was estimated through the Dutch method and the simplified triangular hydrograph method, while the adjustment of the roughness coefficient was considered a valid solution to enhance the drainage capacity of this river mouth.

Keywords: hydraulics; hydrology; insular territories; spatial analysis; territorial management; urban planning

check for updates

Citation: Lousada, S.; Alves, R.; Fernandes, M.; Gonçalves, L. Hydraulic Planning in Insular Urban Territories: The Case of Madeira Island—Ribeira Brava, Tabua. *Water* **2023**, *15*, 2609. https://doi.org/10.3390/w15142609

Academic Editor: Gwo-Fong Lin

Received: 8 June 2023
Revised: 6 July 2023
Accepted: 13 July 2023
Published: 18 July 2023

1. Introduction

Nowadays, a society's sustainable development is significantly influenced by aspects such as weather and climate [1]. For instance, extreme weather conditions are perceived as a risk to the integrity of both the social and economic spheres [1]. As a consequence of the higher level of climate instability, the incidence and intensity of hazardous hydrometeorological phenomena have been increasing [2]. Indeed, the changes in land use, the increase in terms of population density, the geological characteristics, and where a certain region is located are all aspects that can be seen as major contributing factors to most disasters that occur due to climate change [3,4].

In the definition of climate change, one can encompass the variations that occur in terms of the average climatic conditions, either globally or from a regional perspective.

It results from the synergy that arises between the variability that is naturally associated with the climate and all the major modifications in terms of the atmosphere's composition, mainly caused by human actions [5]. Moreover, climate change is currently considered one of the biggest threats to the world [6]. As the temperature rapidly increases due to anthropogenic disturbances, both the patterns of rainfall and the hydrological cycle might end up being altered [7,8]. These alterations in terms of the climate have the capacity to interfere with elements such as temperature and rainfall. In fact, previous studies with observed data [6,7,9] and projected future data [6,8,10] have demonstrated this assumption, especially when it comes to extreme temperature and rainfall events. These rapid changes in climate extremes are believed to cause severe disasters, namely floods and droughts. Hence, studies in this particular field have gathered massive attention globally as the aforementioned aspects enhance the importance of correct planning and management of water resources. Nonetheless, despite being a global phenomenon, extreme changes cannot be seen as homogenous across the world. As such, there are large differences in terms of their frequency and temporal and spatial extent across different regions of the globe [6,11,12]. Hence, to provide different perspectives that account for those differences, it is encouraged for scientists to investigate multiple regions of the world, offering unique perspectives [6].

In recent times, climate experts have been focusing on mitigating the negative impacts of climate extremes, especially in urban areas, since these are areas where studies point out substantial increases in regard to high air temperature extremes [1,13]. However, only approximately 10% of urban areas have been affected by an increase in terms of the frequency of precipitation extremes [1,13]. The positive relationship that exists between the intensity of daily extreme precipitation and global warming is an evidence-based fact. Indeed, it has been determined that the rate of increase is approximately 7% per degree of global warming [1,14]. One other major concern has to do with a scenario where hot and wet extremes meet. For instance, precipitation extremes, when preceded by a heatwave, can have their effects amplified, which ultimately leads to a greater flash flood risk [1,15]. As previously mentioned, these significant climate changes are able to affect temperature and rainfall extremes. Such a scenario has been proven by resorting both to observed data and to simulated future data [6–8]. Considering that such abrupt changes end up leading to severe events, namely floods and droughts, studies whose focus has been directed toward these extremes have received global attention. The increasing attention that this topic has been receiving is related to how much importance aspects such as accurately planning and managing water resources currently have [1,6]. Consequently, decision-makers and policy officials that operate in the field of disaster management have been especially encouraged to develop and implement mitigation and preventive strategies regarding the occurrence of floods. This has occurred mainly due to the changes that took place in the meteorological and socioeconomic fields, which ultimately contributed to an increase in the frequency of this type of phenomenon [4].

Cities are frequently faced with serious and recurring natural disasters, and flooding is an event that can be highlighted among these. Due to the acceleration of the urbanization process, population and economic activities have ended up becoming highly concentrated. This new scenario can be translated into more significant social and economic damages from flooding when compared to the pre-urbanization period [16–18]. Flooding can be classified as the rising or even overflowing of a water flow. Just like droughts and hurricanes, for example, floods are classified as a natural and severe phenomenon. Nevertheless, they can be influenced by a region's characteristics, such as the soil type, the vegetation, and the weather [18,19]. Because of the huge impact that this phenomenon causes, in terms of natural devastation, economic and social losses, and, ultimately, human lives, floods are considered a "natural disaster" [19–21]. Flooding events often result from heavy rainfall, and their effects are mostly felt in urban locations that are disorderly occupied and located in hazardous areas. Indeed, the human need for water resources "forced" cities to be built near rivers [20–23]. Past civilizations looked to establish their cities in the surrounding areas of rivers because of their need for water. This need arose due to multiple purposes, including irrigation, animal necessity, and the assurance of more fertile land [19]. Therefore, one can conclude that urban areas are more prone to be affected by floods not only due to climate change but also as a consequence of an inadequately conducted urbanization process [19,24]. Nevertheless, recent observations point out an increase in terms of the frequency of flooding disasters, mostly because of climate change. In fact, climate change has led to higher levels of annual precipitation and increased runoff from a hydrological perspective; these two factors, when combined, contribute to a higher risk of flooding [4]. As floodings tend to become more recurrent, there has been a growing effort to create accurate flood risk maps. This type of tool arose to sustainably prevent the risks associated with floods and, therefore, protect both the population and the infrastructure [4,25].

Floods are seen as a harmful and recurrent natural disaster that generates obstacles to the socioeconomic development of a significant number of regions worldwide [26–30]. From 1990 to 2016, it is believed that floods all over the globe caused losses of approximately USD 723 billion [17]. Urban areas are the ones that are more prone to be affected by floods, in part due to population growth and climate change, but also because of the increasing intensity and recurrence of these events [31–34]. By 2030, around 40% of all the cities around the globe will be located in regions where the risk of flooding is high, with such a scenario affecting approximately 54 million people [35]. Regarding Southeastern Asia, by 2030, 82% of urban areas will be in high-frequency flood zones [36]. In order to be able to develop accurate risk management plans regarding sustainable land use planning, it is necessary to have a deep understanding of the relationship that exists between floods and urban growth [37,38]. This type of extreme event brings risk mostly to people living either in watercourses' vicinities or in areas with fewer slopes [19–22]. Additionally, the hydrological dynamics of floodplains, rivers, and coastal regions can be influenced by processes that are both natural and of a human-induced nature, which ends up altering aspects such as surface runoff and water infiltration processes [19]. Thus, one can find in floods one of the biggest challenges that humanity will have to face in the near future, especially because of their huge destructive capacity [39,40]. In fact, as the climate in recent years has already been affected by climate change, extreme flood events' frequency has increased, which can be interpreted as a clear and significant threat to humanity [39,41,42].

The flood system has spatial–temporal dynamics, which makes it highly complex, involves uncertainties, and integrates multiple challenges within a system that is responsible for giving rise to complex phenomena [43]. In regard to flood risk management, research assumes a key role in estimating flood hazards and understanding the complex flood risk components, both from an environmental and socioeconomic perspective [44].

The risk that is associated with floods results from a combination of hazards, exposure, and vulnerability. Thus, flood risk management will consist of reducing the damage and/or intensity of the flood [17,22,45–47]. In recent decades, scientific advancements have led to significant alterations regarding the approach utilized to mitigate the negative impacts of floods. Structural measures to control the impacts of floods (e.g., dikes, embankments, etc.) are being substituted by new and more comprehensive models of flood risk management [20,48]. These new approaches consider risk assessment studies—studies that consider flood hazards and exposure/vulnerability factors—to estimate the probabilities and consequences associated with flood events [17,21]. Multiple methodologies have been adopted in order to allow the computation of these indicators. On the one hand, the hazard approaches consider measurement-based data, field surveys [49,50], hydrodynamic models [51,52], and GIS and remote sensing [17,20–22] in the linear modeling of flood risk through overlaying component layers with associated analytical hierarchical process (AHP)-based computed weights. On the other hand, the indicators related to land cover might be divided into two different categories: (i) traditional terrestrial mapping [38,53]; and (ii) land cover classification, which is mostly built around observations via satellites [38,54]. The rise of satellite sensors—for example, Landsat, Satellite Pour Observation de la Terre (SPOT), and Sentinel 2—has been extremely important in enabling a quicker and easier land cover classification as well as in facilitating the study of land cover evolution. Moreover, remote sensing allows a quicker acquisition of data when compared to field survey methods, which also end up being more expensive [55].

The assessment of the risks associated with flooding is a crucial step when defining suitable management strategies [56]. Over the past few decades, studies have concentrated their efforts on developing methodologies for assessing flood risk at multiple scales and considering various goals. Mishra et al. [57] developed an index to analyze the flood propensity of an Indian river, the Kosi River. This index is mostly based on hazards—considering aspects of geomorphologic nature, the distance to the active channel, the slope, and also the levels of rainfall—and on socioeconomic vulnerability. Within the socioeconomic component, they considered aspects such as the population and its characteristics, households, and female densities; levels of literacy; alterations in the cover and use of land; existing intersections between roads and the river; and road density. In addition to this, Chinh Luu et al. [58] studied flood risk's temporal variations. In order to obtain deeper knowledge in regard to this phenomenon's dynamics and to be capable of formulating appropriate strategies of mitigation, this study integrated multiple aspects: the hazard and the level of exposure and vulnerability of a certain region. Dang et al. [59] delineated the key roles required to enhance flood risk assessment methodologies that aim to support the decision-making process. Flood risk indices were divided by the authors into three components: social–economic, physical, and environmental. Kron [60] elaborated on flood risk indices that considered flooding probability and its hypothetical consequences, the social–economic vulnerabilities of the region, and its environment. Begun et al. [17] combined the probability of the occurrence of a flood with the losses that the event would eventually bring. Multiple methodologies aimed at studying flood propensity were developed in several areas. But they have ended up being limited in terms of a comprehensive framework that supports decision-makers in obtaining a better perception of the aggravating risk causes. Additionally, the focus of most of these studies lies in assessing the flood propensity at a specific time. However, Penning-Rowell et al. [61] claim that mitigation measures are more effective when they are evaluated continuously. Jhong et al. [17] reinforce the idea that, to diminish the risk of flooding, understanding the level of vulnerability and hazard at different times is of extreme importance. This is also crucial from a land management perspective since it allows a more accurate analysis of the temporal and spatial trends that are more likely to exist in the future [62].

To assure that a flood study in an urban region will assist in the process of implementing appropriate forecasting and mitigation strategies, it must consider multiple aspects. Indeed, these aspects encompass obtaining topographical data describing the phenomenological processes that are usually associated with flood currents and their interaction with both structures and infrastructure. In addition to that, choosing adequate algorithms to solve model equations is of extreme importance, as it allows results to be obtained [63]. Analyses of this nature must generate so-called hazard and risk maps, i.e., maps that show the final representation of results through graphic products [64].

A major priority regarding the management of urban disasters is to mitigate the negative effects of urban floods [18,65,66]. Since urban flood risk assessments are capable of identifying the probabilities and the main causes associated with the flooding phenomenon, they can be perceived as a key element to prevent and reduce the occurrence of urban floods [18,67–69]. Thus, aiming to prevent significant losses, it becomes fundamental to implement methods that diminish the risk of floods. Multiple factors might be pointed out when discussing the level of vulnerability of a certain region to flood relief characteristics: the compactness coefficient of the watershed, the intensity and distribution of rainfall, the occupation and use of the soil, and the soil type. An approach based on Geographic Information Systems (GIS) enables the determination of the regions that are more susceptible to floods, which can be seen as a great assistance to the decision-making process in this particular field [19,70,71].

Storm sewers, gutters, culverts, tunnels, pipes, detention basins, and other mechanical devices are among the most commonly used measures to control floods [72]. Moreover, advanced gray infrastructure is utilized in some runoff control methods aimed at guiding excess surface flow into disposal and storage sites [73]. However, considering a climate system that in recent times has been severely affected by extreme weather events, these strategies have ended up not being nimble enough to effectively handle large volumes of runoff [74,75]. To improve urban areas' capacity to "resist" floods, different alternative methodologies and concepts have been introduced in different parts of the globe. For instance, low-impact development (LID) in the US [76], sustainable urban drainage systems (SUDS) in the UK [77], water-sensitive urban design (WSUD) in Australia [78], or even the "sponge city" in China [79] are examples of alternative approaches.

A recent report from the European Environment Agency [80] highlighted that a significant number of European nations and organizations have already worked on policies and laws, both at regional and national levels, to enhance cities' adoption of mitigation measures to address the effects of climate change. This strategy is in line with the input of the European Strategy on Adaptation to Climate Change. In addition to the fact that extreme events have become more frequent, the increasing apprehension among all stakeholders has originated a significant focus on this matter. Nonetheless, the changes that occur in terms of land use do not gather that much attention, which may be concerning because if the soil is sealed, the effects of climatic extremes might end up being amplified [81,82].

So, finding new land management strategies assumes a high level of importance. Indeed, the European Strategy outlines the necessity for the member states to define adaptation plans to fight the effects of climate change on a national, regional, and local scale. It is also important to engage municipalities on climate change and to provide all the support needed to implement adaptation measures locally. In fact, the municipal scale has the highest levels of effectiveness, in part due to the fact that municipalities are responsible for managing land use through urban planning [81].

Regarding land planning, two important lines of study arise: (i) the analysis and adoption of mitigation strategies after the events occurred; (ii) the increment in terms of the territory's resilience, in order to allow it to more easily adapt to the new scenarios that might end up arising as a result of the aforementioned changes and, therefore, mitigate risks that may derive from them, considering that more permeable soils can be translated into soils that are more prepared for absorbing heavy rain [38,81].

Consequently, prevention assumes a crucial role in both scenarios and can be achieved by appropriately planning and designing the territory. The fact is that management and solutions end up having multiple approaches, and there is a need to integrate them. Here, planning is particularly relevant, as this step focuses precisely on the root causes of the problems as well as preventive measures [38,81].

Based on this, the current study conducts a hydrological analysis focused on this particular region to estimate the expected peak flow rate, considering a time of recurrence of 100 years. With this a posteriori knowledge, we establish a comparison between this value and the drainage capacity that this watershed's stream mouth possesses. After demonstrating that the mouth's hydraulic characteristics are not enough to drain the estimated peak flow rate, it is necessary to size a detention basin as a mitigation measure aiming to normalize the flow downstream. The ultimate goal is to allow the mouth to operate normally, considering the dimensions that it currently has. Moreover, this study also focuses on the need for structural actions in the region of the mouth, a measure that, it is worth saying, would not implicate significant urban impacts. This structural intervention would be associated with an alteration of the physical features of the stream's riverbed and walls, namely, the coefficient of roughness. Thus, to increase the drainage capacity, the minimum characteristics of the stream end up being verified without the necessity of dimensional changes.

2. Materials and Methods

2.1. Area of Study

This study analyzes the Tabua (Ribeira Brava) watershed, which is located on Madeira island's southern slope, latitude 32°40′ N and longitude 17°50′ W [23,83]. It belongs to the Ribeira Brava municipality and acts as the precipitation catchment area, supplying one of the municipality's main streams, as can be seen in Figure 1. Madeira is an island in the archipelago of Madeira, Portugal, located in the Atlantic Ocean (north zone), belonging to the so-called Macaronesia Region, close to Europe and Africa.

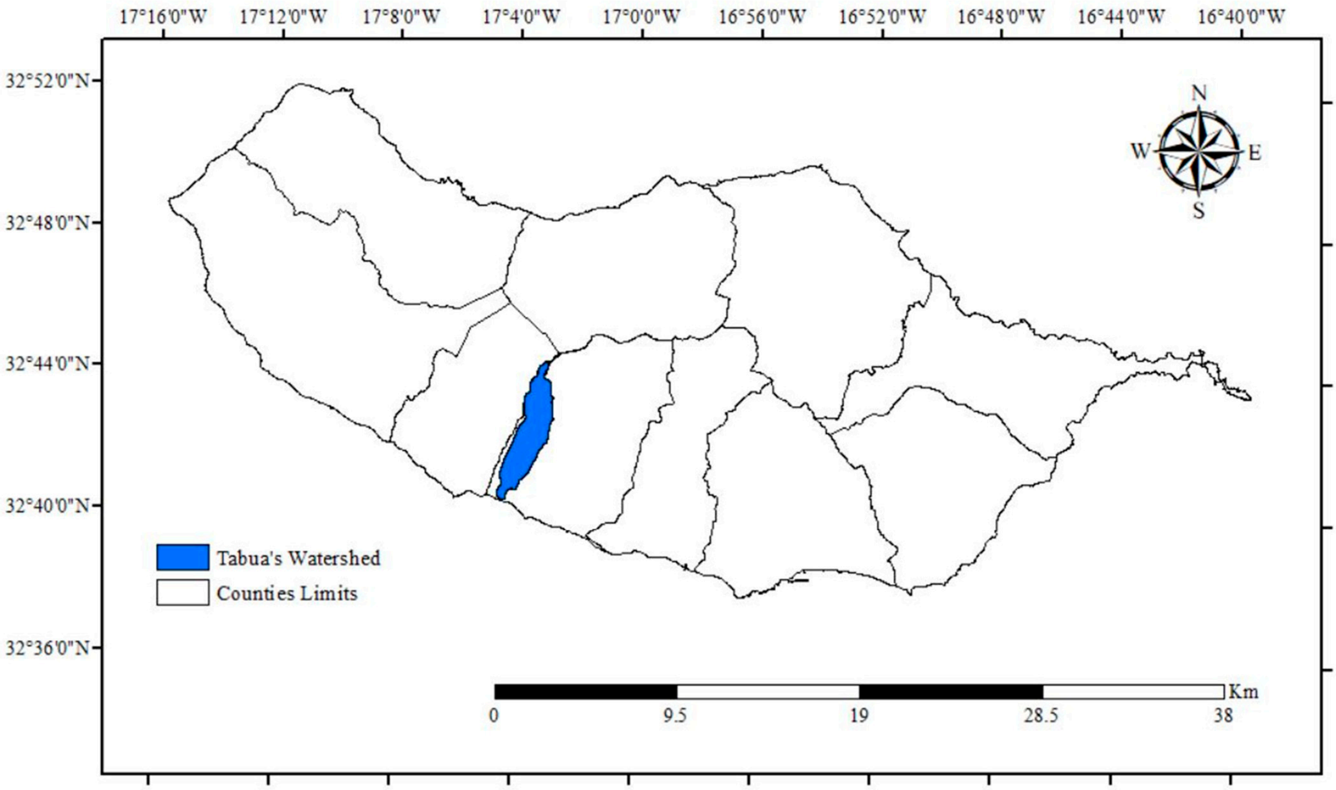

Figure 1. The Tabua (Ribeira Brava) watershed (Source: authors by ESRI ArcGIS, 2020).

Similar to Funchal, which is Madeira's main municipality, this watershed is significantly exposed to flooding events, as observed both in 2010 and 2013, when flooding provoked serious losses from material and human perspectives. As the Tabua (Ribeira Brava) watershed is located in an area with significantly high levels of urbanization, this region's soil has a relatively high rate of sealing, mostly due to the presence of buildings and pavements [20,23]. Additionally, as is demonstrated in Figure 2, the presence of vegetation and sedimentation in this watershed's river mouth needs to be considered since it reduces the channel's drainage capacity.

The level of conservation of the stream is significantly homogeneous throughout the part of its length that is located in the urban area and might be confirmed in situ. Its reduced slope can be seen as the main cause of the excess sedimentation and vegetation, which ultimately results in a slower drainage process and contributes to drag sediments with a larger grain size.

Figure 2. Observation of the study area: state of conservation of Tabua (Ribeira Brava) main watercourse river mouth (from east to river mouth) (Source: authors).

2.2. Schematic of the Methodology

The methodology that was adopted in this study is divided into 6 stages, as Figure 3 shows.

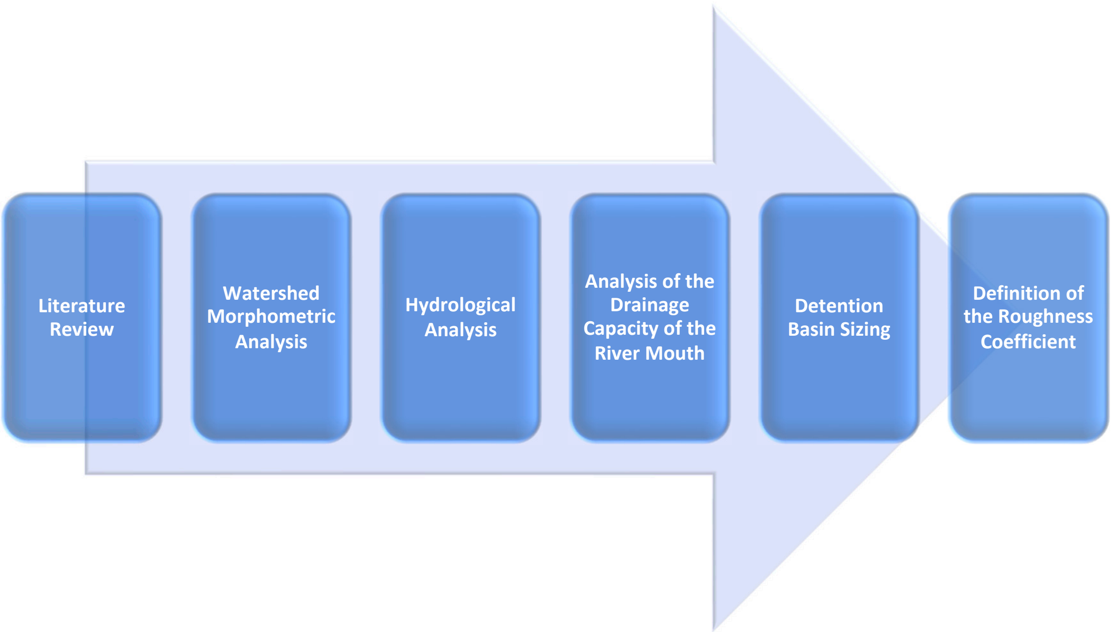

Figure 3. Organogram of the adopted methodology.

This study's approach started with an intensive review of the literature, aiming to collect the largest possible amount of important information to assure a precise characterization of this basin, both from a morphometric and hydrological perspective. Hence, after conducting the literature review mentioned above, the methodologies suggested by different authors were considered in order to conduct a flood propensity analysis with a satisfactory level of reliability. Finally, the steps mentioned in Figure 3 are depicted below.

2.3. Morphometric Characterization of the Watershed

Regarding a watershed's morphometric characterization, the key parameters to be used are the following [84–87]:

- **Gravelius Index—K_C:** The relationship between the perimeters of the basin under study and a perfectly circular one—both with identical areas—was utilized to estimate the level of similarity of the watershed's geometric shape to a perfect circle [86]. This parameter can be obtained through Equation (1). Considering that this is a dimensionless parameter, a value close to "1" can be translated into a watershed whose shape will be similar to a perfect circle, regardless of its dimensions; as watersheds with rounded shapes tend to present higher levels of flood propensity, values closer to "1" will be associated with a greater risk regarding this type of phenomenon [86]. Therefore, we will have the following classifications for K_C: 1.00–1.25, basin with high propensity for large floods; 1.25–1.50, basin with medium tendency to large floods; >1.50, basin not subject to large floods.

$$K_C = P/2 \times \sqrt{\pi \times A} \tag{1}$$

where

P = watershed's perimeter, in "km";
A = area of the watershed, in "km^2".

- **Elongation Factor—K_L:** The relationship between the watershed being analyzed and a rectangle—both with identical areas—was used to estimate the elongation of the watershed, regardless of its dimensions. This can be obtained by resorting to Equation (2). If a certain watershed has an elongation factor higher than "2", it can be classified as an elongated one [86].

$$K_L = \frac{L_E}{l_E} = \frac{\frac{K_C \times \sqrt{A}}{1.128} \times \left| 1 + \sqrt{1 - \left(\frac{1.128}{K_C}\right)^2} \right|}{\frac{K_C \times \sqrt{A}}{1.128} \times \left| 1 - \sqrt{1 - \left(\frac{1.128}{K_C}\right)^2} \right|} \tag{2}$$

where

L_E = equivalent length, in "km";
l_E = equivalent width, in "km";
K_C = Gravelius index, a dimensionless parameter, in "/";
A = area of the watershed, in "km^2".

- **Shape Factor—K_F:** Relates to the watershed's average length and width. This parameter can be obtained through Equation (3). Lower values are associated with more elongated watersheds—and, therefore, with watersheds where the risk of flooding is lower—regardless of their size. Additionally, if the value is close to "1", then the basin's format will be similar to a square. Therefore, we will have the following classifications for K_F: 1.00–0.75, basin with high propensity for large floods; 0.75–0.50, basin with medium tendency to large floods; <0.50, basin not subject to large floods.

$$K_F = A/{L_B}^2 \tag{3}$$

where

A = area of the watershed, in "km^2";
L_B = watershed's length, in "km".

The length of a given watershed might be estimated using the distance between the stream's mouth and its furthest point. Nonetheless, it is worth mentioning that a watershed's length does not necessarily have to be equal to its main watercourse's length. Some variations between these two values might arise as a result of the larger size that the main watercourse tends to have, mostly because of its sinuosity. Resorting to the MDE file, which was provided by LREC-RAM (the Regional Civil Engineering Laboratory of the Autonomous Region of Madeira), it was possible to conduct a morphological characterization of both the Tabua (Ribeira Brava) watershed and its main watercourse. In order to avert restrictions associated with using a single method, the data that were gathered during this study were utilized in the equations of various authors.

First, to conduct a morphometric analysis, it was necessary to establish a hierarchy based on the order and magnitude of the watercourses; for that reason, both the Strahler and the Shreve classifications were utilized [87]. Indeed, these two classifications can be estimated by conducting a hydrological analysis of the DEM file, a process that involves obtaining the "flow direction" and "flow accumulation" rasters through the "flow order" tool [20]. Additionally, studies point out that the Strahler classification is highly connected with a watershed's ratio of branching/bifurcation. Equation (4) allows the estimation of each degree of branching or bifurcation [20,21,84,86].

$$R_B = \frac{N_i}{N_{i+1}} \tag{4}$$

where

N_i = number of watercourses classified as "i", a dimensionless parameter, in "/";

N_{i+1} = number of watercourses classified as "i + 1", a dimensionless parameter, in "/";

This can be obtained by dividing the number of watercourses in a certain order by the number of watercourses encompassed in the order immediately above, regardless of their dimensions. Moreover, the average level of bifurcation is obtained based on Equation (5).

$$\overline{R_B} = \sqrt[i-1]{\prod_{i=1}^{i-1} \frac{N_i}{N_{i+1}}} = \sqrt[i-1]{N_1} \tag{5}$$

where

N_i = number of watercourses classified as "i", a dimensionless parameter, in "/";

N_{i+1} = number of watercourses classified as "i + 1", a dimensionless parameter, in "/";

N_1 = number of first-order watercourses.

As this parameter only denotes the arithmetic mean of bifurcation ratios, it is also dimensionless. Additionally, a key aspect for the accurate morphometric characterization of any watershed is its concentration time. This parameter indicates the time that the watershed's total area needs to contribute to the drainage process that will culminate in the stream's mouth [20,21,84,86,87].

Considering that the equations utilized to calculate the time of concentration are empirical, different methodologies might end up with varying results for the same parameter. Therefore, in order to avert extreme results, it is advisable to calculate the arithmetic mean. In this case, the arithmetic mean was calculated using the results derived from the methodologies of Kirpich, Témez, and Giandotti (Equations (6)–(8), respectively) [86,88].

$$t_C = 57 \times \left(L^3/(H_{MAX} - H_{MIN})\right)^{0.385} \tag{6}$$

where

t_C = concentration time, in "minutes";

L = main watercourse's length, in km;

H_{MAX} = main watercourse's maximum height, in "m";

H_{MIN} = main watercourse's minimum height, in "m".

$$t_C = \left(\frac{L}{i^{0.25}}\right)^{0.76} \quad (7)$$

where

t_C = concentration time, in "hours";
L = main watercourse's length, in "km";
i = main watercourse's slope, in "m/m".

$$t_C = \frac{\left(4 + \sqrt{A}\right) + (1.5 \times L)}{0.8 \times \sqrt{H_M}} \quad (8)$$

where

t_C = concentration time, in "hours";
A = area of the watershed, in "km^2";
L = main watercourse's length, in "km";
H_M = watershed's average height, in "m".

2.4. Precipitation Analysis

The precipitation analysis that was conducted in this research was based on a probabilistic analysis regarding short-term extreme events. As such, in order to enable this analysis, data were gathered from public sources, namely precipitation-related information automatically recorded by the National Water Resources Information System (SNIRH) (period of sixteen years). The Gumbel distribution was selected here because it was the probabilistic methodology that would better fit the already acquired data and the anticipated forecasts for the watersheds located in Madeira [20,21]. Hence, Equation (9) can be utilized to estimate the annual maximum daily precipitation.

$$P_{EST} = P_M + S' \times K_T \quad (9)$$

where

P_{EST} = estimated maximum annual daily precipitation, in "mm";
P_M = average annual daily precipitation, in "mm";
S' = standard deviation of the sample, in "mm;"
K_T = frequency factor, a dimensionless parameter, in "/".
And

$$S' = \left(\frac{\sum(X_i - X_M)^2}{n'}\right)^{0.5} \quad (10)$$

where

X_i = sample value, in "mm";
X_M = sample mean, in "mm";
n' = number of samples.

$$K_T = -\frac{6^{0.5}}{\pi} \times \left\{0.577216 + \ln\left(\ln\left(\frac{T_R}{T_R - 1}\right)\right)\right\} \quad (11)$$

where

T_R = return period, in "years".

Therefore, given a certain duration, the intensity of the precipitation might be determined utilizing Equation (12).

$$I = \frac{P_{EST} \times k}{t_C} \quad (12)$$

where

I = intensity of the precipitation, in "mm/h";
P_{EST} = estimated maximum annual daily precipitation, in "mm";
t_C = concentration time, in "hours";
k = coefficient of time distribution, a dimensionless parameter, in "/".
And

$$k = 0.181 \times \ln(t_C) + 0.4368 \quad (13)$$

where
t_C = concentration time, in "hours".

Given that the annual maximum daily precipitation is applicable only to events that last an entire day, the coefficient of time distribution assumes key importance. Thus, since a watershed's concentration time is equal to the duration of the precipitation event, if one were to utilize the total level of daily precipitation, it would ultimately result in oversized hydraulic structures [86,88].

2.5. Drainage Capacity of the River Mouth and Peak Flow Rate

The Manning–Strickler equation presented in Equation (14) was utilized to calculate the stream mouth's capacity of drainage; then, a comparison was made between the value obtained and the projected flow considering an extreme event for a period of recurrence of 100 years. Moreover, to estimate the projected flow, multiple methodologies that had a significant level of support among researchers were utilized, namely: Forti, Rational, Giandotti, and Mockus (Equations (16)–(19), respectively).

$$Q_M = \left(\frac{1}{n}\right) \times A_M \times R^{\frac{2}{3}} \times \sqrt{i} \quad (14)$$

where
Q_M = stream mouth's capacity of drainage, in "m^3/s".
A_M = area of the river mouth cross-section, in "m^2";
R = hydraulic radius, in "m";
i = river mouth's average slope, in "m/m";
n = coefficient of roughness of the riverbed and walls, in "$m^{-1/3}$ s", Table A1.
And

$$R = \frac{B + 2 \times h}{A_M} \quad (15)$$

where
B = river mouth runoff section's width, in "m";
h = river mouth runoff section's height, in "m";
A_M = area of the river mouth cross-section, in "m^2".

It is worth mentioning that previous studies that focused on this area were used as the main base to gather information regarding aspects such as the stream's height and width in the mouth area [86]. In fact, the confirmation of this first parameter was possible due to the utilization of the georeferencing process.

$$Q_{Forti} = A \times \left(b \times \frac{500}{125 + A}\right) + c \quad (16)$$

where
Q_{Forti} = peak flow rate by Forti, in "m^3/s";
A = area of the watershed, in "km^2";

b = for this parameter, the value "2.35" was considered for maximum daily precipitation below 200 "mm" and the value "3.25" for levels above 200 "mm";

c = for this parameter, the value "0.5" was considered for maximum daily precipitation below 200 "mm" and the value "1" for levels above 200 "mm".

$$Q_{Rational} = \frac{C \times I \times A}{3.6} \quad (17)$$

where

$Q_{Rational}$ = peak flow rate by the rational methodology, in "m^3/s";
C = coefficient of surface runoff, Table A2;
I = intensity of the precipitation, in "mm/h";
A = area of the watershed, in "km^2".

$$Q_{Giandotti} = \frac{\lambda \times A \times P_{MAX}}{t_C} \tag{18}$$

where

$Q_{Giandotti}$ = peak flow rate by Giandotti, in "m^3/s";
λ = reduction coefficient, Table A3;
A = area of the watershed, in "km^2";
P_{MAX} = height of precipitation considering a duration identical to the time of concentration, in "mm";
t_C = concentration time, in "hours".

$$Q_{Mockus} = \frac{2.08 \times A \times P_{EST} \times C}{\sqrt{t_C} + 0.6 \times t_C} \tag{19}$$

where

Q_{Mockus} = peak flow rate by Mockus, in "m^3/s";
A = area of the watershed, in "km^2";
P_{EST} = level of precipitation estimated, in "cm";
C = coefficient of surface runoff, Table A2;
t_C = concentration time, in "hours".

In order to guarantee that the population is secure, the dimensions of hydraulic structures have to consider a fill rate below 85% [86,89]. Hence, the implementation of mechanisms that enable the regulation of the runoff, for instance, spillways, assumes a significant level of importance.

As previously mentioned, Equation (20) is used to calculate the fill rate. If the mouth has not enough drainage capacity to deal with the level of rain flow that exists in the watershed and cannot assure that the safety margin is accomplished, it becomes necessary to estimate the dimensions of accurate structures of mitigation, like detention basins.

$$FR = \frac{Q_P}{Q_M} \times 100 \tag{20}$$

where

FR = fill rate, in "%";
Q_P = each methodology's peak flow rate, in "m^3/s";
Q_M = stream mouth's capacity of drainage, in "m^3/s".

The fill rate is related to a given section's capacity for drainage regarding a certain flow. Therefore, in a scenario where this parameter is greater than 100%, the section is not capable of dealing with such a high level of water, which ultimately leads to overflow [86].

2.6. Detention Basin Sizing

As previously mentioned, in scenarios where the mouth is not capable of handling the volume of rainwater, it becomes necessary to dimension a spillway in order to guarantee the normalization of the flow that will ultimately reach the stream's mouth. In this case, a spillway of the Cipolleti type was picked due to its capacity to facilitate runoff and reduce turbulence in areas where there is contact with water [85,90]. Its dimensions were calculated utilizing Equation (21).

Once the flow to be drained to the mouth was established and regulated, it became possible to calculate the level of water that the detention basin would retain. To determine this level of water, two approaches were considered: the Dutch method and the simplified triangular hydrograph (STH) method (Equations (22) and (23), respectively).

$$Q_S = 1.86 \times L_{SD} \times {H_D}^{1.5} \quad (21)$$

where

Q_S = flow drained by spillway, in "m^3/s";
L_{SD} = sill's width, in "m^3/s";
H_D = height of the waterline above the sill, in "m".

$$V_A = (Q_P - Q_S) \times t_C \times 3600 \quad (22)$$

$$V_A = \frac{(Q_P - Q_S) \times (2 \times t_C - 2 \times [Q_S/\{Q_P/t_C\}])}{2} \quad (23)$$

where

V_A = volume of storage, in "m^3";
Q_P = each methodology's peak flow rate, in "m^3/s";
Q_S = flow drained by the spillway, in "m^3/s";
t_C = concentration time, in "hours".

It should be noted that the base for Equation (23) can be found in the STH's geometric examination (Figure A1). Indeed, this equation was established by taking into account an event that lasts at least twice as long as a watershed's time of concentration. Considering that the last particle of rainwater to reach the stream's mouth would originate from the farthest point and would be generated in the last moment of the precipitation event, it becomes clear that it would be necessary to consider the value of the concentration time for the volume drained by the river mouth [86].

Given that the Dutch method fails to account for the damping and delay of the precipitation hydrograph, the hydraulic structures whose dimensions are estimated considering this methodology might end up being oversized [91], as Figure 4 demonstrates, where q_s is the spillway's runoff capacity; t_c is the time of concentration; t_{MAX} is the maximum duration of precipitation (base); t_d is the time delay until the process of accumulation of water starts in the detention basin; $H_{a,MAX}$ is the maximum capacity of storage; i(t_{MAX}) is the intensity of precipitation associated with the maximum duration.

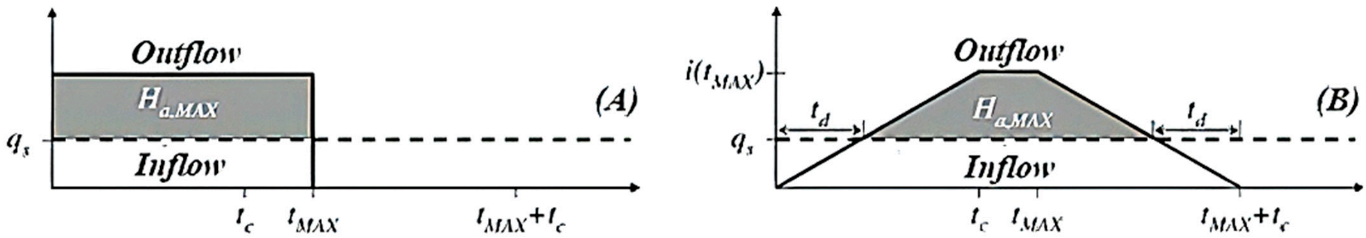

Figure 4. (**A**) Dutch method; (**B**) STH method (Source: [27]).

Thus, it was demonstrated that, when resorting to the Dutch method, the storage process and precipitation initiate at the same time, which is an unrealistic scenario given that storage will not begin until the moment when the flow drained downstream exceeds the spillway's runoff capacity.

2.7. Modification of the Roughness Coefficient

Additionally, from a structural perspective, as a mitigation strategy, the alteration of the coefficient of roughness of the watercourse's riverbed and walls was considered. One of the most significant advantages associated with this measure is that it enhances the capacity of drainage by diminishing the friction level. This measure consists of modifying the value associated with the "n" parameter in the Manning–Strickler equation with the aim of enhancing a certain watercourse's flow, which might be accomplished by changing the material that covers both the stream's riverbed and walls [86].

3. Results

The values that are presented in this section correspond to the results generated by the application of the aforementioned formulas. Thus, in order to assess the morphometric traits of this watershed's principal watercourse, it became necessary to conduct an individual analysis that focused on the parameters presented in Table 1, establishing correlations with reference values recommended by various authors.

Table 1. Parameters calculated or extracted from ArcGIS.

Parameter	Measurement Unit	Result
Area	km^2	8.809
Perimeter	km	22.530
Main watercourse's length	km	9.272
Main watercourse's maximum height	m	1547.650
Main watercourse's minimum height	m	0.000
Average time of concentration	hours	1.409
Gravelius coefficient of compactness	dimensionless	2.141
Elongation factor	dimensionless	12.334
Shape factor	dimensionless	0.151
Number of watercourses	units	335.000
Average bifurcation ratio	dimensionless	4.172
Strahler classification	dimensionless	4.000

The first parameter analyzed, which is related to the watershed's area, has a significant level of relevance when studying the water volume drained to the mouth. Moreover, considering its area, a watershed can be classified as: very large > 20 km^2; large > 10 km^2; medium > 1 km^2; and small < 1 km^2 [92]. In line with what the table above illustrates, this watershed can be classified as "Small", which can be translated into a lower propensity to flooding when compared to larger watersheds. Nonetheless, it is worth mentioning that reference values tend to be arbitrary; therefore, they may end up differing in accordance with the type of analysis that is being performed [92].

This watershed's borders have higher altitudes when compared to its central region, as Figure 5 demonstrates, which indicates a steep slope that will enhance a rapid supply to the main course, originating higher volumes of water in the stream and, ultimately, in the river mouth.

In regard to this watershed's system of drainage, illustrated in Figure 6, the presence of numerous watercourses—mostly medium- or even low-order watercourses that end up supplying the principal watercourse—is associated with a larger drainage capacity. In fact, this indicator can be interpreted as the behavior of a certain area, hydrographically speaking, which has as its key aspect the probability of generating new watercourses. In basins with larger hydric densities, there is a greater tendency to generate new watercourses, and, as a consequence, these basins usually have a larger number of ephemeral channels [86,87].

To conduct a precipitation analysis, it was necessary to resort to the data from the National Information System on Water Resources (SNIRH) [93], as this platform gathers data over a period of sixteen years. This data can be observed in Table A4 and Figure A2 (daily maximums). Thus, the Gumbel distribution's probabilistic processing allowed the acquisition of the values that are present in Table 2.

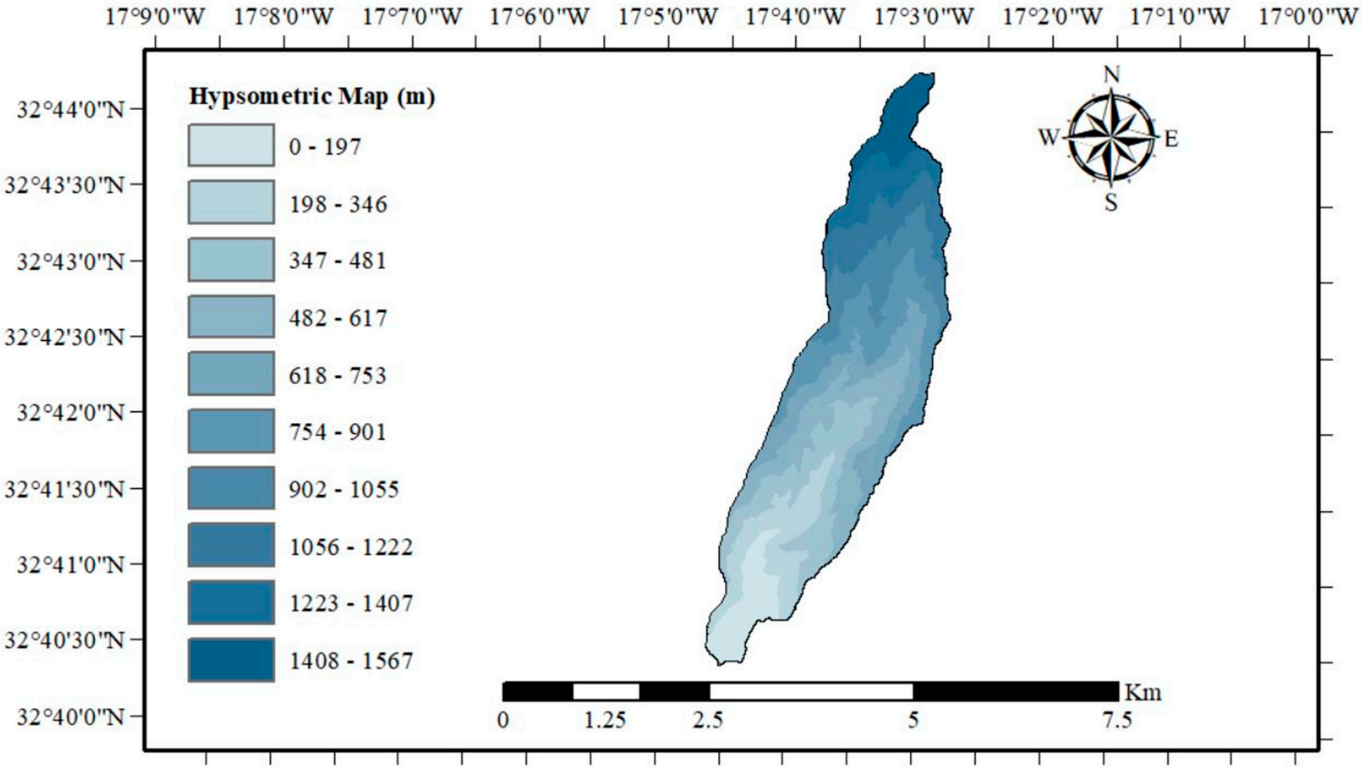

Figure 5. Hypsometric map of Tabua's watershed: DEM file (Source: authors, by ESRI ArcGIS, 2020).

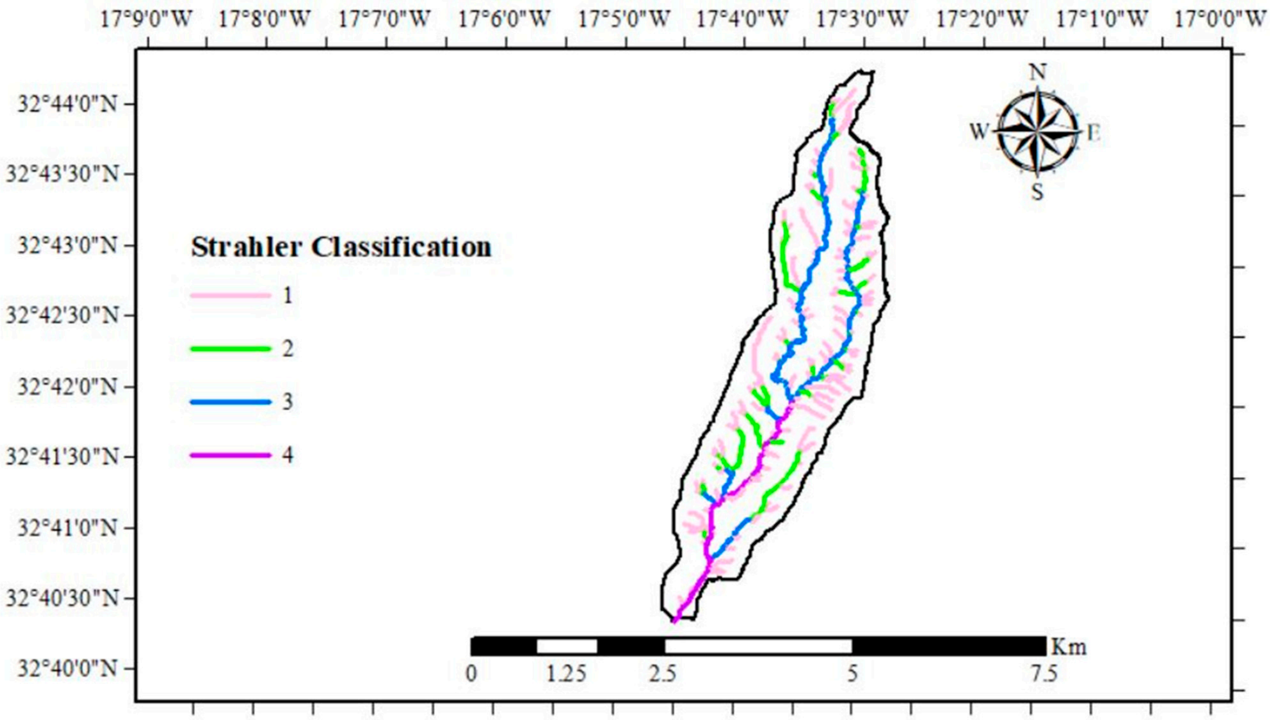

Figure 6. Strahler classification of Tabua's watershed (Source: authors by ESRI ArcGIS, 2020).

Table 2. Precipitation parameters.

Parameter	Symbol	Measurement Unit	Result
Average annual precipitation	P_M	mm	164.443
Standard deviation	S'	mm	64.424
Frequency factor	K_T	dimensionless	3.136
Coefficient of time distribution	k	dimensionless	0.592
Maximum annual daily precipitation	P_{EST}	mm	366.521
Precipitation intensity	I	mm/h	91.920

Subsequently, the peak flow rates were calculated using the formulas that were mentioned in the previous section (Equations (16)–(19)), as shown in Table 3; this was possible because the precipitation intensity for a recurrence time of 100 years had already been determined. Regarding the surface drainage coefficient, a value of 0.500 was utilized in the rational methodology (Table 4) since the region in which the study is focused can be classified as a peripheral area with commercial buildings. In other words, this value is associated with the parcel of water that is usually drained superficially, that is, half of the total precipitation.

Table 3. Peak flow rate.

Methodology	Flow (m^3/s)
Forti	115.787
Rational	95.355
Giandotti	201.727
Mockus	165.218

Table 4. Surface drainage coefficient adopted (Source: [94]).

Urban Areas		
Occupation of the Land		**Coefficient of Surface Drainage**
Commercial area	City center	0.700–0.950
	Peripheral areas	**0.500**–0.700

In order to estimate the flow utilizing Giandotti's methodology, the value presented in Table 5 was adopted for the reduction coefficient (λ).

Table 5. Adopted Giandotti's reduction coefficient (Source: [95]).

Area (km^2)	λ	Equivalent "C"
<300	0.346	1.250

In terms of the river mouth's capacity for drainage, it became necessary to resort to the Manning–Stickler equation to analyze whether a detention basin would be necessary in this case or not; the results gathered in this process can be found in Table 6. Nonetheless, it is relevant to point out that the bed and walls of the stream do not have the same coefficients of roughness. Hence, the river mouth's capacity for drainage was calculated through a weighted mean, considering the respective coefficients. Regarding the stream walls, since they present a satisfactory condition, n = 0.020; on the contrary, the stream bed is in a poorer condition, with a surface partly covered by vegetation, boulders, and pebbles, which implicates n = 0.040 (Table A1). One other crucial aspect lies in the fact that the river mouth region has a remarkably low scope, which is usually associated with a deceleration of the water flow and a decrease in terms of the capacity of drainage. In order to simulate a critical scenario, a 0.01 m/m slope was considered in the reference section.

Table 6. Assessment of the need for detention basin implementation.

Parameter	Measurement Unit	Result
River mouth's width	m	10.000
River mouth's height	m	3.000
River mouth's capacity for drainage	m^3/s	140.359
Fill rate—Forti (pre-regularization)	%	82
Fill rate—Rational (pre-regularization)	%	68
Fill rate—Giandotti (pre-regularization)	%	144
Fill rate—Mockus (pre-regularization)	%	118

Table 6 shows that both the Giandotti and the Mockus methodologies exceeded the limit of 85% for the fill rate. So, it became necessary to define and implement flow control and mitigation measures in the river mouth area. Based on that assumption, the sizing of a detention basin was carried out, taking into account the methodologies referred to above while also considering the spatial and urban limitations associated with the existing infrastructure located in the stream's surroundings.

Since the detention basin's dimensions depend on the exceeding flow, a Cipolletti trapezoid spillway's size was estimated, aiming to regularize and control the flow that will end up draining downstream. The characteristics of the spillway are listed in Table 7.

Table 7. Application of the Cipolletti spillway.

Parameter	Measurement Unit	Result
Spillway's width	m	8.500
Height of the spillway sill	m	3.00
Outflow of the spillway	m^3/s	82.151
Fill rate—Giandotti (post-regularization)	%	59
Fill rate—Mockus (post-regularization)	%	59

After that, both the Dutch method and the STH method were utilized to estimate the dimensions of the detention basins. These methodologies have as one of their most significant drawbacks the fact that they are considered simplified approaches as they do not consider multiple factors; consequently, the use of these methodologies might result in an overestimation of this structure. Moreover, aiming to diminish the implementation works' environmental and urban impacts, the detention basin's height and width were fixed, as they were set considering the existing cross-section values. Thus, the structure's length was the only geometric variable; nevertheless, this variable is limited by the main watercourse's length.

After resorting to the previously mentioned methodologies, it became possible to obtain the results presented in Table 8.

Table 8. Detention basin sizing.

Parameter	Measurement Unit	Result
Width	m	10.000
Height	m	3.000
Length—Dutch method (Giandotti)	m	20,217.169
Length—STH method (Giandotti)	m	11,983.932
Length—Dutch method (Mockus)	m	14,044.453
Length—STH method (Mockus)	m	7061.140

Lastly, the alteration of the roughness coefficient was also considered since this measure would mitigate the flooding effects while simultaneously keeping the riverbed vegetation intact. So, Table 9 displays values that are related to the improvement in the conservation level of the riverbed, with the objective of enhancing its drainage capacity by reducing the friction that exists between the covering material and the fluid.

Table 9. Modification of the roughness coefficient.

Parameter	Measurement Unit	Result
Wall roughness coefficient—modified	$m^{-1/3}$	0.012
Riverbed roughness coefficient—modified	$m^{-1/3}$	0.030
Drainage capacity of the river mouth—modified	m^3/s	196.200
Fill rate—Rational (post-modification)	%	49
Fill rate—Giandotti (post-modification)	%	103
Fill rate—Mockus (post-modification)	%	84

To sum up, the altered walls' coefficients of roughness are related to the surface with concrete finishing in good condition, notwithstanding the fact that the riverbed maintains its stony and vegetated features, although in good condition. Table 10 shows the values associated with these coefficients.

Table 10. Adopted roughness coefficient (Source: [95]).

Channel Typology of the Channel	Very Good	Good	Regular	Bad
Channel with a vegetated and stony slope	0.025	**0.030**	0.035	0.040
Concrete finishing surface	0.011	**0.012**	0.013	0.015

4. Discussion

Since this study's main objective was to analyze the necessity of implementing simplified mitigation measures in the watershed under study, the detention basin was revealed to be an efficient measure to control the flow in the river mouth area; this strategy can be classified as a structural measure [86]. Indeed, the fill rate dropped to 59% as a result of this mitigation measure, while, initially, the fill rate was superior to any of the other methodologies: Forte (82%), Rational (68%), Giandotti (144%), and Mockus (118%). Hence, it has been demonstrated that the detention basin enables the river mouth to operate significantly below the 85% limit that was previously mentioned. In addition, this study is in line with the analysis that was undertaken by the Regional Directorate for Territorial Ordering and Environment (DROTA), as Table 11 demonstrates, which is a positive indicator regarding this study's level of accuracy.

Table 11. Watersheds with high flood risk (Source: [96]).

Municipality	Watershed
Ribeira Brava	Ribeira Brava Tabua

One of the objectives of this study was to find mitigation measures that did not cause significant impacts, either in the waterway or its surroundings. This objective was selected due to the fact that natural elements and values located in cities are key to the environmental recovery of an urban region [97]. Moreover, urban and natural systems are coexistent, which means that their type of management needs to be an integrated one as it is a regional space requirement and has significant importance for a region's sustainability [98,99]. If not, a disorganized urbanization process might lead to urban voids [100].

Therefore, the streams' cross-section dimensions were not altered, resulting in length as the only dimensional variable. Considering that fact, the utilization of the Dutch method originated in oversized results, as the total length of the detention basin surpassed the length that the main waterway possesses. As a result, it would be necessary to modify one of the other dimensions, such as height or width. So, in this scenario, the Dutch method cannot provide a satisfactory level of accuracy for the urban conditions that were imposed.

Regarding the STH method, it could be applied in this case because the detention basin's total length is shorter in comparison with the main watercourse's length.

In terms of the roughness coefficient alteration, the final decision was to preserve the riverbed's stony and vegetated characteristics since the main focus would be enhancing its level of conservation. In addition to that, this decision was also based on the fact that removing the entirety of the sediments, vegetation, boulders, and pebbles located in the riverbed is a strategy that would involve multiple costs (monetary costs, time spent, etc.). As for the walls, frequent maintenance is not needed due to the fact that wear by abrasion would take place in an alluvial channel that has a greater tendency for draining high volumes of water in addition to large granular sediments.

The alteration of the roughness coefficient, despite being considered a simple mitigation measure, had satisfactory effects (with the exception of Giandotti's methodology), which enabled the river mouth to avoid working above the filling limit. In fact, the STH method and the alteration of the coefficient of roughness can be adopted simultaneously, and that would lead to a detention basin with a reduced length and, therefore, with an optimized dimension.

Nonetheless, these simplified methodologies do not take into account local specificities. This results in an excessive safety margin that will ultimately cause oversized structures.

5. Conclusions

This study's main results point out the flood susceptibility of the Tabua (Ribeira Brava) watershed if an extreme precipitation event were to take place, as reported by DROTA in their Flood Risk Report. One of the most significant contributing factors to this is the presence of vegetation, boulders, and pebbles on the stream bed's surface, diminishing its runoff capacity. This also contributes to the deceleration of the water flow, which ultimately reduces the capacity of drainage; this can especially be verified in areas with lower slopes, for instance, the river mouth. Indeed, the fact that the mouth's capacity for drainage here analyzed was insufficient ended up being sustained by two out of four of the utilized methodologies: Mockus and Giandotti.

In terms of the simplified mitigation measures that were proposed, the Dutch method suggested a length for the detention basin that was longer than the main watercourse's length; this led to the conclusion that this methodology could not be applied in a scenario like this. In contrast, the simplified triangular hydrograph method enabled the implementation of this structure without modifying the stream's width and/or height.

Lastly, the promotion of alterations regarding the roughness coefficient also generated positive effects regarding flood mitigation. This can be seen as even more satisfactory in the sense that this measure is relatively simple to implement.

As it is unfeasible to consider all the aspects that constitute a more accurate and complete study in this case, further analyses can be undertaken to complement or reinforce the results obtained. For instance, studies that focus on the capacity of drainage of the implemented urban hydraulic system, aiming to decrease the volume stored on the detention basins; analyses that consider the deposition of sediments, considering the main watercourse's entrainment velocity [101]; monitoring of the level of deterioration presented by the walls of the artificial canal as a result of abrasion and the estimation of the recommended time for maintenance (processes of desilting and silting); the impacts of the quality of the water discharged on the artificial water channel's degradation process [102,103]; study of projections related to the growth of urban areas in the region here analyzed and whether that process will end up influencing the increase in the flow; analyses aiming to estimate the costs associated with the establishment of the mitigation strategies suggested by this analysis; studies on the impacts of the tide level in an artificial channel's process of drainage and whether there is a connection with the probability of downstream floods occurring or not; and studying the effects that this type of channel has regarding territorial planning, i.e., adaptation considering rural watersheds.

The results obtained in this study reinforce the conclusions that similar analyses—that also resorted to simulations and case study analysis as the main drivers for scientific development—present [104,105].

Author Contributions: Conceptualization, S.L., R.A., M.F. and L.G.; methodology, S.L.; software, S.L. and L.G.; validation, S.L. and L.G.; formal analysis, S.L. and L.G.; investigation, S.L.; resources, L.G.; data curation, S.L. and L.G.; writing—original draft preparation, S.L., R.A., M.F. and L.G.; writing—review and editing, S.L.; visualization, R.A., M.F. and L.G.; supervision, R.A., M.F. and L.G.; project administration, S.L. All authors have read and agreed to the published version of the manuscript.

Funding: Through the funding provided by CONSTRUTEAM ENGENHARIA LDA, we were able to obtain the necessary resources to conduct the research, analyze relevant data, and draft this article. Furthermore, the trust and investment in our work demonstrate the recognition of the value and potential of this research. We hope that this enduring partnership continues to promote research and development in the field of civil construction. Once again, we are deeply grateful to CONSTRUTEAM ENGENHARIA LDA for the invaluable support.

Institutional Review Board Statement: Not applicable.

Informed Consent Statement: Not applicable.

Data Availability Statement: The data presented in this study are openly available. Also, it is possible to contact one of the study authors.

Acknowledgments: Special thanks are due to CONSTRUTEAM ENGENHARIA LDA, Civil Construction Company, for the generous financial support granted, which made this study and article publication possible. The significant contribution was fundamental to the success of this research project. We would like to express our sincere gratitude to CONSTRUTEAM ENGENHARIA LDA for the continuous support in advancing scientific knowledge within the field of civil construction. Without this sponsorship, this publication would not have been possible.

Conflicts of Interest: The authors declare no conflict of interest.

Appendix A

Table A1. Manning–Strickler roughness coefficients (Source: [95]).

Channel Type and Description	Very Good	Good	Regular	Bad
Mortared stone masonry	0.017	0.020	0.025	0.030
Rigged stone masonry	0.013	0.014	0.015	0.017
Dry stone masonry	0.025	0.033	0.033	0.035
Brick masonry	0.012	0.013	0.015	0.017
Smooth metal gutters (semicircular)	0.011	0.012	0.013	0.016
Open channels in rock (irregular)	0.035	0.040	0.045	-
Channels with bottom on land and slope with stones	0.028	0.030	0.033	0.035
Channels with stony bed and vegetated slope	0.025	0.030	0.035	0.040
Channels with concrete coating	0.012	0.014	0.016	0.018
Earth channels (rectilinear and uniform)	0.017	0.020	0.023	0.025
Dredged canals	0.025	0.028	0.030	0.033
Clay conduits (drainage)	0.011	0.012	0.014	0.017
Vitrified clay conduits (sewage)	0.011	0.013	0.015	0.017
Flattened wooden plank conduits	0.010	0.012	0.013	0.014
Gabion	0.022	0.030	0.035	-
Cement mortar surfaces	0.011	0.012	0.013	0.015
Smoothed cement surfaces	0.010	0.011	0.012	0.013

Table A1. *Cont.*

Channel Type and Description	Very Good	Good	Regular	Bad
Cast iron coated tube with tar	0.011	0.012	0.013	-
Uncoated cast iron pipe	0.012	0.013	0.014	0.015
Brass or glass tubes	0.009	0.010	0.012	0.013
Concrete pipes	0.012	0.013	0.015	0.016
Galvanized iron pipes	0.013	0.014	0.015	0.017
Rectilinear and uniform clean streams and rivers	0.025	0.028	0.030	0.033
Streams and rivers cleared, rectilinear and uniform with stones and vegetation	0.030	0.033	0.035	0.040
Streams and rivers cleared, rectilinear and uniform with intricacies and wells	0.035	0.040	0.045	0.050
Spread margins with little vegetation	0.050	0.060	0.070	0.080
Spread margins with lots of vegetation	0.075	0.100	0.125	0.150

Table A2. Surface runoff coefficients (Source: [94]).

Urban Areas		
Occupation of the Land		**Coefficient of Surface Runoff**
Green areas	Lawns on sandy soils	0.050–0.200
	Lawns on heavy soils	0.150–0.350
	Parks and cemeteries	0.100–0.350
	Sports fields	0.200–0.350
Commercial areas	City district	0.700–0.950
	Periphery	0.500–0.700
Residential areas	Town-center villas	0.300–0.500
	Villas on the outskirts	0.250–0.400
	Apartment buildings	0.500–0.700
Industrial areas	Dispersed industry	0.500–0.800
	Concentrated industry	0.600–0.900
Railways		0.200–0.400
Streets and roads	Paved	0.700–0.900
	Concrete	0.800–0.950
	In brick	0.700–0.850

Table A3. Giandotti reduction coefficients (Source: [95]).

A (km^2)	λ	"C" Equivalent
<300	0.346	1.250
300–500	0.277	1.000
500–1000	0.197	0.710
1000–8000	0.100	0.360
8000–20,000	0.076	0.270
20,000–70,000	0.055	0.200

Table A4. Precipitation historical data (Source: [93]).

n	Year	(mm)
1	1998/1999	170.000
2	1999/2000	180.700
3	2000/2001	135.000
4	2001/2002	190.000
5	2002/2003	195.400
6	2003/2004	141.000
7	2004/2005	103.200
8	2005/2006	91.400
9	2006/2007	141.400
10	2007/2008	104.600

Table A4. *Cont.*

n	Year	(mm)
11	2008/2009	155.000
12	2009/2010	257.800
13	2010/2011	148.400
14	2011/2012	288.600
15	2012/2013	267.400
16	2013/2014	61.200

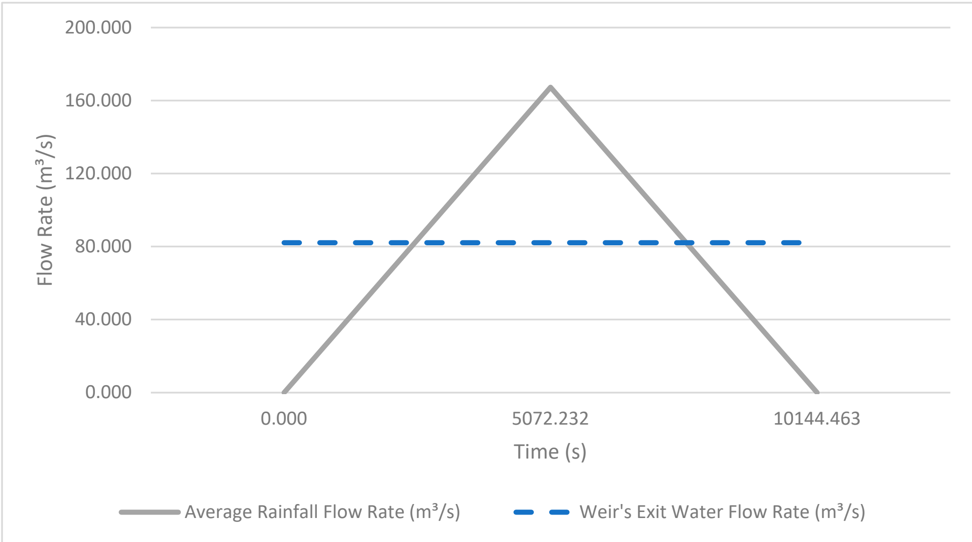

Figure A1. Ternary phase diagram.

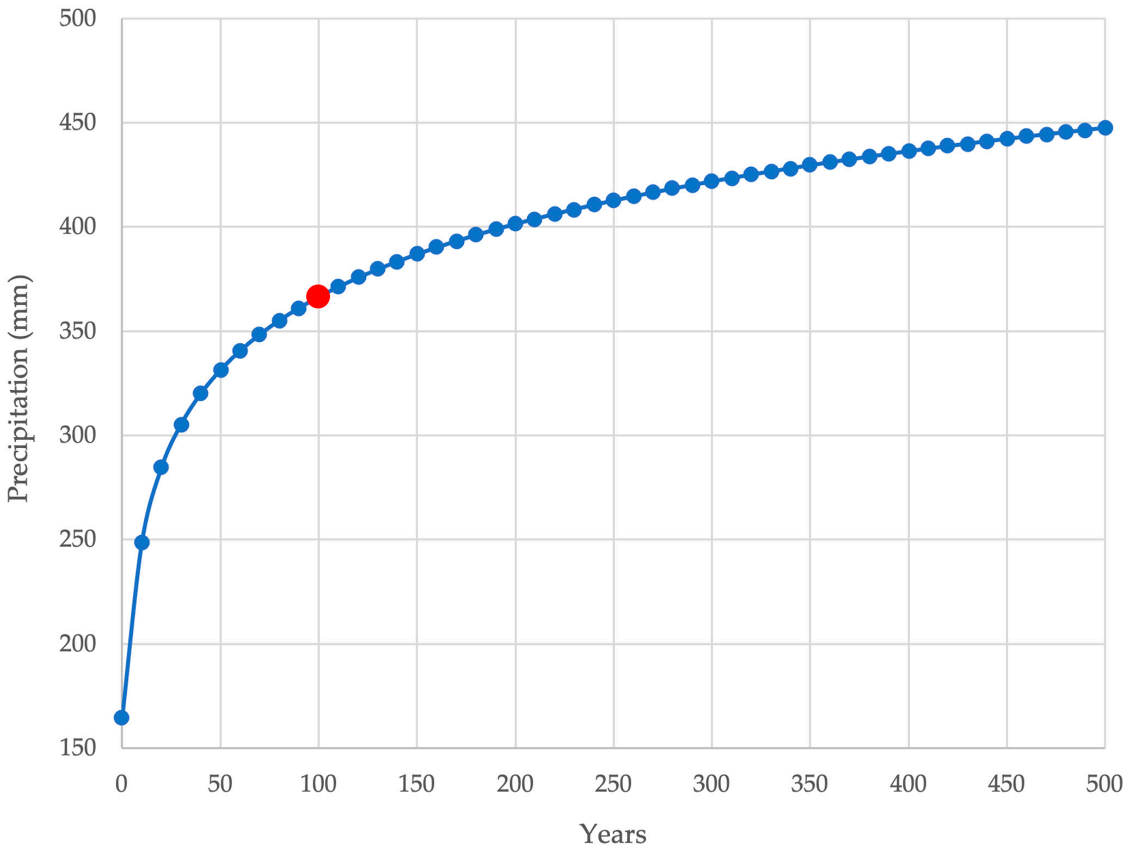

Figure A2. Expected rainfall for Tabua (Ribeira Brava) watershed.

References

1. Evstigneev, V.P.; Naumova, V.A.; Voronin, D.Y.; Kuznetsov, P.N.; Korsakova, S.P. Severe Precipitation Phenomena in Crimea in Relation to Atmospheric Circulation. *Atmosphere* **2022**, *13*, 1712. [CrossRef]
2. Coumou, D.; Robinson, A. Historic and Future Increase in the Global Land Area Affected by Monthly Heat Extremes. *Environ. Res. Lett.* **2013**, *8*, 034018. [CrossRef]
3. Diaz, J.H. Global Climate Changes, Natural Disasters, and Travel Health Risks. *J. Travel Med.* **2006**, *13*, 361–372. [CrossRef] [PubMed]
4. Ighile, E.H.; Shirakawa, H.; Tanikawa, H. Application of GIS and Machine Learning to Predict Flood Areas in Nigeria. *Sustainability* **2022**, *14*, 5039. [CrossRef]
5. Pinna, M.S.; Loi, M.C.; Calderisi, G.; Fenu, G. Extremes Rainfall Events on Riparian Flora and Vegetation in the Mediterranean Basin: A Challenging but Completely Unexplored Theme. *Water* **2022**, *14*, 817. [CrossRef]
6. Das, S.; Kamruzzaman, M.; Islam, A.R.M.T.; Zhu, D.; Kumar, A. Comparison of Future Changes in Frequency of Climate Extremes between Coastal and Inland Locations of Bengal Delta Based on CMIP6 Climate Models. *Atmosphere* **2022**, *13*, 1747. [CrossRef]
7. Fowler, H.J.; Ali, H.; Allan, R.P.; Ban, N.; Barbero, R.; Berg, P.; Blenkinsop, S.; Cabi, N.S.; Chan, S.; Dale, M.; et al. Towards Advancing Scientific Knowledge of Climate Change Impacts on Short-Duration Rainfall Extremes. *Philos. Trans. R. Soc. Math. Phys. Eng. Sci.* **2021**, *379*, 20190542. [CrossRef]
8. Tang, B.; Hu, W.; Duan, A. Future Projection of Extreme Precipitation Indices over the Indochina Peninsula and South China in CMIP6 Models. *J. Clim.* **2021**, *34*, 8793–8811. [CrossRef]
9. Papalexiou, S.M.; Montanari, A. Global and Regional Increase of Precipitation Extremes Under Global Warming. *Water Resour. Res.* **2019**, *55*, 4901–4914. [CrossRef]
10. Frías, M.D.; Mínguez, R.; Gutiérrez, J.M.; Méndez, F.J. Future Regional Projections of Extreme Temperatures in Europe: A Nonstationary Seasonal Approach. *Clim. Change* **2012**, *113*, 371–392. [CrossRef]
11. Kharin, V.V.; Zwiers, F.W.; Zhang, X.; Wehner, M. Changes in Temperature and Precipitation Extremes in the CMIP5 Ensemble. *Clim. Change* **2013**, *119*, 345–357. [CrossRef]
12. Tebaldi, C.; Hayhoe, K.; Arblaster, J.M.; Meehl, G.A. Going to the Extremes. *Clim. Change* **2006**, *79*, 185–211. [CrossRef]
13. Mishra, V.; Ganguly, A.R.; Nijssen, B.; Lettenmaier, D.P. Changes in Observed Climate Extremes in Global Urban Areas. *Environ. Res. Lett.* **2015**, *10*, 024005. [CrossRef]
14. Hodnebrog, Ø.; Marelle, L.; Alterskjær, K.; Wood, R.R.; Ludwig, R.; Fischer, E.M.; Richardson, T.B.; Forster, P.M.; Sillmann, J.; Myhre, G. Intensification of Summer Precipitation with Shorter Time-Scales in Europe. *Environ. Res. Lett.* **2019**, *14*, 124050. [CrossRef]
15. Chen, Y.; Liao, Z.; Shi, Y.; Li, P.; Zhai, P. Greater Flash Flood Risks From Hourly Precipitation Extremes Preconditioned by Heatwaves in the Yangtze River Valley. *Geophys. Res. Lett.* **2022**, *49*, e2022GL099485. [CrossRef]
16. Hemmati, M.; Ellingwood, B.R.; Mahmoud, H.N. The Role of Urban Growth in Resilience of Communities Under Flood Risk. *Earths Future* **2020**, *8*, e2019EF001382. [CrossRef]
17. Nguyen, H.D.; Fox, D.; Dang, D.K.; Pham, L.T.; Viet Du, Q.V.; Nguyen, T.H.T.; Dang, T.N.; Tran, V.T.; Vu, P.L.; Nguyen, Q.-H.; et al. Predicting Future Urban Flood Risk Using Land Change and Hydraulic Modeling in a River Watershed in the Central Province of Vietnam. *Remote Sens.* **2021**, *13*, 262. [CrossRef]
18. Wu, Z.; Xue, W.; Xu, H.; Yan, D.; Wang, H.; Qi, W. Urban Flood Risk Assessment in Zhengzhou, China, Based on a D-Number-Improved Analytic Hierarchy Process and a Self-Organizing Map Algorithm. *Remote Sens.* **2022**, *14*, 4777. [CrossRef]
19. Carvalho, R.d.C.F.; Moreira, T.R.; de Souza, K.B.; Costa, G.A.; Zanetti, S.S.; Barbosa, K.V.; Filho, C.B.C.; Miranda, M.R.; Guerra Filho, P.A.; dos Santos, A.R.; et al. GIS-Based Approach Applied to Study of Seasonal Rainfall Influence over Flood Vulnerability. *Water* **2022**, *14*, 3731. [CrossRef]
20. Lousada, S.; Cabezas, J.; Castanho, R.A.; Gómez, J.M.N. Hydraulic Planning in Insular Urban Territories: The Case of Madeira Island—Ribeira Brava. *Water* **2021**, *13*, 2951. [CrossRef]
21. Lousada, S.; Gonçalves, L.; Atmaca, A. Hydraulic Planning in Insular Urban Territories: The Case of Madeira Island—São Vicente. *Water* **2022**, *14*, 112. [CrossRef]
22. Lousada, S.; Castanho, R.A. GIS-Based Assessment of Morphological and Hydrological Parameters of Ribeira Dos Socorridos and Ribeira Do Vigario Basins, Madeira Island, Portugal. *Curr. World Environ.* **2021**, *16*, 408–426. [CrossRef]
23. Lousada, S.A.N.; Moura, A.D.S.; Gonçalves, L.B. Numerical modelling of the flow rate in artificial water channels: Application to Ribeira Brava's stream. *Rev. Bras. Planej. E Desenvolv.* **2020**, *9*, 39–59. [CrossRef]
24. Berndtsson, R.; Becker, P.; Persson, A.; Aspegren, H.; Haghighatafshar, S.; Jönsson, K.; Larsson, R.; Mobini, S.; Mottaghi, M.; Nilsson, J.; et al. Drivers of Changing Urban Flood Risk: A Framework for Action. *J. Environ. Manag.* **2019**, *240*, 47–56. [CrossRef]
25. Danso-Amoako, E.; Scholz, M.; Kalimeris, N.; Yang, Q.; Shao, J. Predicting Dam Failure Risk for Sustainable Flood Retention Basins: A Generic Case Study for the Wider Greater Manchester Area. *Comput. Environ. Urban Syst.* **2012**, *36*, 423–433. [CrossRef]
26. Marchand, M.; Buurman, J.; Pribadi, A.; Kurniawan, A. Damage and Casualties Modelling as Part of a Vulnerability Assessment for Tsunami Hazards: A Case Study from Aceh, Indonesia. *J. Flood Risk Manag.* **2009**, *2*, 83–147. [CrossRef]
27. Pradhan, B.; Youssef, A.M. A 100-Year Maximum Flood Susceptibility Mapping Using Integrated Hydrological and Hydrodynamic Models: Kelantan River Corridor, Malaysia. *J. Flood Risk Manag.* **2011**, *4*, 189–202. [CrossRef]

28. Dawod, G.M.; Mirza, M.N.; Al-Ghamdi, K.A. GIS-Based Estimation of Flood Hazard Impacts on Road Network in Makkah City, Saudi Arabia. *Environ. Earth Sci.* **2012**, *67*, 2205–2215. [CrossRef]
29. Robi, M.A.; Abebe, A.; Pingale, S.M. Flood Hazard Mapping under a Climate Change Scenario in a Ribb Catchment of Blue Nile River Basin, Ethiopia. *Appl. Geomat.* **2019**, *11*, 147–160. [CrossRef]
30. Francesch-Huidobro, M.; Dabrowski, M.; Tai, Y.; Chan, F.; Stead, D. Governance Challenges of Flood-Prone Delta Cities: Integrating Flood Risk Management and Climate Change in Spatial Planning. *Prog. Plan.* **2017**, *114*, 1–27. [CrossRef]
31. Carter, J.G. Urban Climate Change Adaptation: Exploring the Implications of Future Land Cover Scenarios. *Cities* **2018**, *77*, 73–80. [CrossRef]
32. Stoleriu, C.C.; Urzica, A.; Mihu-Pintilie, A. Improving Flood Risk Map Accuracy Using High-Density LiDAR Data and the HEC-RAS River Analysis System: A Case Study from North-Eastern Romania. *J. Flood Risk Manag.* **2020**, *13*, e12572. [CrossRef]
33. Iosub, M.; Minea, I.; Chelariu, O.E.; Ursu, A. Assessment of Flash Flood Susceptibility Potential in Moldavian Plain (Romania). *J. Flood Risk Manag.* **2020**, *13*, e12588. [CrossRef]
34. Huţanu, E.; Mihu-Pintilie, A.; Urzica, A.; Paveluc, L.E.; Stoleriu, C.C.; Grozavu, A. Using 1D HEC-RAS Modeling and LiDAR Data to Improve Flood Hazard Maps Accuracy: A Case Study from Jijia Floodplain (NE Romania). *Water* **2020**, *12*, 1624. [CrossRef]
35. Güneralp, B.; Seto, K.C. Futures of Global Urban Expansion: Uncertainties and Implications for Biodiversity Conservation. *Environ. Res. Lett.* **2013**, *8*, 014025. [CrossRef]
36. Güneralp, B.; Güneralp, İ.; Liu, Y. Changing Global Patterns of Urban Exposure to Flood and Drought Hazards. *Glob. Environ. Change* **2015**, *31*, 217–225. [CrossRef]
37. Ran, J.; Nedovic-Budic, Z. Integrating Spatial Planning and Flood Risk Management: A New Conceptual Framework for the Spatially Integrated Policy Infrastructure. Comput. Environ. *Urban Syst.* **2016**, *57*, 68–79. [CrossRef]
38. Lousada, S.; Cabezas, J.; Castanho, R.A.; Gómez, J.M.N. Land-Use Changes in Insular Urban Territories: A Retrospective Analysis from 1990 to 2018. The Case of Madeira Island—Ribeira Brava. *Sustainability* **2022**, *14*, 16839. [CrossRef]
39. Xu, C.; Yang, J.; Wang, L. Application of Remote-Sensing-Based Hydraulic Model and Hydrological Model in Flood Simulation. *Sustainability* **2022**, *14*, 8576. [CrossRef]
40. Dottori, F.; Szewczyk, W.; Ciscar, J.-C.; Zhao, F.; Alfieri, L.; Hirabayashi, Y.; Bianchi, A.; Mongelli, I.; Frieler, K.; Betts, R.A.; et al. Author Correction: Increased Human and Economic Losses from River Flooding with Anthropogenic Warming. *Nat. Clim. Change* **2018**, *8*, 1021. [CrossRef]
41. Rehman, S.; Sahana, M.; Hong, H.; Sajjad, H.; Ahmed, B.B. A Systematic Review on Approaches and Methods Used for Flood Vulnerability Assessment: Framework for Future Research. *Nat. Hazards* **2019**, *96*, 975–998. [CrossRef]
42. Mateo-Garcia, G.; Veitch-Michaelis, J.; Smith, L.; Oprea, S.V.; Schumann, G.; Gal, Y.; Baydin, A.G.; Backes, D. Towards Global Flood Mapping Onboard Low Cost Satellites with Machine Learning. *Sci. Rep.* **2021**, *11*, 7249. [CrossRef] [PubMed]
43. Lin, K.; Chen, H.; Xu, C.-Y.; Yan, P.; Lan, T.; Liu, Z.; Dong, C. Assessment of Flash Flood Risk Based on Improved Analytic Hierarchy Process Method and Integrated Maximum Likelihood Clustering Algorithm. *J. Hydrol.* **2020**, *584*, 124696. [CrossRef]
44. Yang, W.; Xu, K.; Lian, J.; Bin, L.; Ma, C. Multiple Flood Vulnerability Assessment Approach Based on Fuzzy Comprehensive Evaluation Method and Coordinated Development Degree Model. *J. Environ. Manag.* **2018**, *213*, 440–450. [CrossRef]
45. Koks, E.E.; Jongman, B.; Husby, T.G.; Botzen, W.J.W. Combining Hazard, Exposure and Social Vulnerability to Provide Lessons for Flood Risk Management. *Environ. Sci. Policy* **2015**, *47*, 42–52. [CrossRef]
46. Vojtek, M.; Vojteková, J. Flood Maps and Their Potential Role in Local Spatial Planning: A Case Study from Slovakia. *Water Policy* **2018**, *20*, 1042–1058. [CrossRef]
47. Meyer, V.; Scheuer, S.; Haase, D. A Multicriteria Approach for Flood Risk Mapping Exemplified at the Mulde River, Germany. *Nat. Hazards* **2009**, *48*, 17–39. [CrossRef]
48. Meyer, V.; Haase, D.; Scheuer, S. Flood Risk Assessment in European River Basins—Concept, Methods, and Challenges Exemplified at the Mulde River. *Integr. Environ. Assess. Manag.* **2009**, *5*, 17–26. [CrossRef]
49. Luu, C.; Von Meding, J.; Kanjanabootra, S. Assessing Flood Hazard Using Flood Marks and Analytic Hierarchy Process Approach: A Case Study for the 2013 Flood Event in Quang Nam, Vietnam. *Nat. Hazards* **2018**, *90*, 1031–1050. [CrossRef]
50. Chau, V.N.; Holland, J.; Cassells, S.; Tuohy, M. Using GIS to Map Impacts upon Agriculture from Extreme Floods in Vietnam. *Appl. Geogr.* **2013**, *41*, 65–74. [CrossRef]
51. Teng, J.; Jakeman, A.J.; Vaze, J.; Croke, B.F.W.; Dutta, D.; Kim, S. Flood Inundation Modelling: A Review of Methods, Recent Advances and Uncertainty Analysis. *Environ. Model. Softw.* **2017**, *90*, 201–216. [CrossRef]
52. Fewtrell, T.J.; Duncan, A.; Sampson, C.C.; Neal, J.C.; Bates, P.D. Benchmarking Urban Flood Models of Varying Complexity and Scale Using High Resolution Terrestrial LiDAR Data. *Phys. Chem. Earth Parts ABC* **2011**, *36*, 281–291. [CrossRef]
53. Talukdar, S.; Singha, P.; Mahato, S.; Shahfahad; Pal, S.; Liou, Y.-A.; Rahman, A. Land-Use Land-Cover Classification by Machine Learning Classifiers for Satellite Observations—A Review. *Remote Sens.* **2020**, *12*, 1135. [CrossRef]
54. Akodéwou, A.; Oszwald, J.; Saïdi, S.; Gazull, L.; Akpavi, S.; Akpagana, K.; Gond, V. Land Use and Land Cover Dynamics Analysis of the Togodo Protected Area and Its Surroundings in Southeastern Togo, West Africa. *Sustainability* **2020**, *12*, 5439. [CrossRef]
55. Wittke, S.; Yu, X.; Karjalainen, M.; Hyyppä, J.; Puttonen, E. Comparison of Two-Dimensional Multitemporal Sentinel-2 Data with Three-Dimensional Remote Sensing Data Sources for Forest Inventory Parameter Estimation over a Boreal Forest. *Int. J. Appl. Earth Obs. Geoinf.* **2019**, *76*, 167–178. [CrossRef]

56. De Moel, H.; Jongman, B.; Kreibich, H.; Merz, B.; Penning-Rowsell, E.; Ward, P.J. Flood Risk Assessments at Different Spatial Scales. *Mitig. Adapt. Strateg. Glob. Change* **2015**, *20*, 865–890. [CrossRef]
57. Mishra, K.; Sinha, R. Flood Risk Assessment in the Kosi Megafan Using Multi-Criteria Decision Analysis: A Hydro-Geomorphic Approach. *Geomorphology* **2020**, *350*, 106861. [CrossRef]
58. Luu, C.; Tran, H.X.; Pham, B.T.; Al-Ansari, N.; Tran, T.Q.; Duong, N.Q.; Dao, N.H.; Nguyen, L.P.; Nguyen, H.D.; Thu Ta, H.; et al. Framework of Spatial Flood Risk Assessment for a Case Study in Quang Binh Province, Vietnam. *Sustainability* **2020**, *12*, 3058. [CrossRef]
59. Dang, N.M.; Babel, M.S.; Luong, H.T. Evaluation of Food Risk Parameters in the Day River Flood Diversion Area, Red River Delta, Vietnam. *Nat. Hazards* **2011**, *56*, 169–194. [CrossRef]
60. Kron, W. Flood Risk = Hazard · Values · Vulnerability. *Water Int.* **2005**, *30*, 58–68. [CrossRef]
61. Penning-Rowsell, E.C.; Yanyan, W.; Watkinson, A.R.; Jiang, J.; Thorne, C. Socioeconomic scenarios and flood damage assessment methodologies. *J. Flood Risk Manag.* **2013**, *6*, 23–32. [CrossRef]
62. Mechler, R.; Bouwer, L.M. Understanding Trends and Projections of Disaster Losses and Climate Change: Is Vulnerability the Missing Link? *Clim. Change* **2015**, *133*, 23–35. [CrossRef]
63. Hirabayashi, Y.; Mahendran, R.; Koirala, S.; Konoshima, L.; Yamazaki, D.; Watanabe, S.; Kim, H.; Kanae, S. Global Flood Risk under Climate Change. *Nat. Clim. Change* **2013**, *3*, 816–821. [CrossRef]
64. Gambardella, C.; Parente, R.; Scotto di Santolo, A.; Ciaburro, G. New Digital Field of Drawing and Survey for the Automatic Identification of Debris Accumulation in Flooded Areas. *Sustainability* **2023**, *15*, 479. [CrossRef]
65. Wang, P.; Li, Y.; Yu, P.; Zhang, Y. The Analysis of Urban Flood Risk Propagation Based on the Modified Susceptible Infected Recovered Model. *J. Hydrol.* **2021**, *603*, 127121. [CrossRef]
66. Huang, H.; Chen, X.; Zhu, Z.; Xie, Y.; Liu, L.; Wang, X.; Wang, X.; Liu, K. The Changing Pattern of Urban Flooding in Guangzhou, China. *Sci. Total Environ.* **2018**, *622–623*, 394–401. [CrossRef]
67. Dhiman, R.; VishnuRadhan, R.; Eldho, T.I.; Inamdar, A. Flood Risk and Adaptation in Indian Coastal Cities: Recent Scenarios. *Appl. Water Sci.* **2018**, *9*, 5. [CrossRef]
68. Zhao, L.; Zhang, T.; Fu, J.; Li, J.; Cao, Z.; Feng, P. Risk Assessment of Urban Floods Based on a SWMM-MIKE21-Coupled Model Using GF-2 Data. *Remote Sens.* **2021**, *13*, 4381. [CrossRef]
69. Zhou, Y.; Shen, D.; Huang, N.; Guo, Y.; Zhang, T.; Zhang, Y. Urban Flood Risk Assessment Using Storm Characteristic Parameters Sensitive to Catchment-Specific Drainage System. *Sci. Total Environ.* **2019**, *659*, 1362–1369. [CrossRef]
70. Cai, T.; Li, X.; Ding, X.; Wang, J.; Zhan, J. Flood Risk Assessment Based on Hydrodynamic Model and Fuzzy Comprehensive Evaluation with GIS Technique. *Int. J. Disaster Risk Reduct.* **2019**, *35*, 101077. [CrossRef]
71. Costache, R.; Trung Tin, T.; Arabameri, A.; Crăciun, A.; Ajin, R.S.; Costache, I.; Reza Md Towfiqul Islam, A.; Abba, S.I.; Sahana, M.; Avand, M.; et al. Flash-Flood Hazard Using Deep Learning Based on H_2O R Package and Fuzzy-Multicriteria Decision-Making Analysis. *J. Hydrol.* **2022**, *609*, 127747. [CrossRef]
72. Dhakal, K.P.; Chevalier, L.R. Urban Stormwater Governance: The Need for a Paradigm Shift. *Environ. Manag.* **2016**, *57*, 1112–1124. [CrossRef]
73. Omitaomu, O.A.; Kotikot, S.M.; Parish, E.S. Planning Green Infrastructure Placement Based on Projected Precipitation Data. *J. Environ. Manag.* **2021**, *279*, 111718. [CrossRef]
74. Montz, B.E.; Tobin, G.A. Livin' Large with Levees: Lessons Learned and Lost. *Nat. Hazards Rev.* **2008**, *9*, 150–157. [CrossRef]
75. Ahern, J. From Fail-Safe to Safe-to-Fail: Sustainability and Resilience in the New Urban World. *Landsc. Urban Plan.* **2011**, *100*, 341–343. [CrossRef]
76. Eckart, K.; McPhee, Z.; Bolisetti, T. Performance and Implementation of Low Impact Development–A Review. *Sci. Total Environ.* **2017**, *607–608*, 413–432. [CrossRef]
77. Li, L.; Collins, A.M.; Cheshmehzangi, A.; Chan, F.K.S. Identifying Enablers and Barriers to the Implementation of the Green Infrastructure for Urban Flood Management: A Comparative Analysis of the UK and China. *Urban For. Urban Green.* **2020**, *54*, 126770. [CrossRef]
78. Duan, Y.; Gao, Y.G.; Zhang, Y.; Li, H.; Li, Z.; Zhou, Z.; Tian, G.; Lei, Y. "The 20 July 2021 Major Flood Event" in Greater Zhengzhou, China: A Case Study of Flooding Severity and Landscape Characteristics. *Land* **2022**, *11*, 1921. [CrossRef]
79. Nguyen, T.T.; Ngo, H.H.; Guo, W.; Wang, X.C.; Ren, N.; Li, G.; Ding, J.; Liang, H. Implementation of a Specific Urban Water Management-Sponge City. *Sci. Total Environ.* **2019**, *652*, 147–162. [CrossRef] [PubMed]
80. Urban Adaptation in Europe—European Environment Agency. Available online: https://www.eea.europa.eu/publications/urban-adaptation-in-europe (accessed on 1 March 2023).
81. Leone, A.; Grassini, L.; Balena, P. Urban Planning and Sustainable Storm Water Management: Gaps and Potential for Integration for Climate Adaptation Strategies. *Sustainability* **2022**, *14*, 16870. [CrossRef]
82. Pelorosso, R.; Leone, A.; Boccia, L. Land Cover and Land Use Change in the Italian Central Apennines: A Comparison of Assessment Methods. *Appl. Geogr.* **2009**, *29*, 35–48. [CrossRef]
83. Tabua. Wikipédia Enciclopédia Livre 2021. Available online: https://pt.wikipedia.org/w/index.php?title=Tabua&oldid=62166432 (accessed on 3 March 2023).
84. Tucci, C.E.M. *Gestão de Águas Pluviais Urbanas*; Universidade Federal do Rio Grande do Sul (UFRGS): Rio Grande do Sul, Brazil, 1993; p. 270.

85. Gonçalves, L.B.; Lousada, S.A.N. Análise Probabilística de Cheias e o Uso de Bacias de Detenção como Medida Mitigadora: Aplicação à Bacia de Santa Luzia. *Rev. Científica Monfragüe Desarro. Resiliente: Extremadura, Spain* **2020**, *13*.
86. Lousada, S.A.N.; Camacho, R.F. *Hidrologia, Recursos Hídricos E Ambiente: Aulas Teóricas*; Universidade da Madeira: Funchal, Madeira, Portugal, 2018; Volume 1, ISBN 978-989-8805-33-1.
87. Geomorfologia-Antonio Christofoletti.Pdf. Available online: https://toaz.info/doc-view (accessed on 28 March 2022).
88. Taboni, B.; Licata, M.; Buleo Tebar, V.; Bonasera, M.; Umili, G. Proposal for Flood Risk Mitigation in the Upper Tanaro Valley (Western Alps—North-Western Italy). *Geosciences* **2022**, *12*, 260. [CrossRef]
89. Tucci, C.E.M.; Porto, R.L.; Barros, M.T. *Drenagem Urbana*; Universidade Federal do Rio Grande do Sul (UFRGS): Rio Grande do Sul, Brazil, 1995; 414p.
90. Vieira, I.; Barreto, V.; Figueira, C.; Lousada, S.; Prada, S. The Use of Detention Basins to Reduce Flash Flood Hazard in Small and Steep Volcanic Watersheds—A Simulation from Madeira Island. *J. Flood Risk Manag.* **2018**, *11*, S930–S942. [CrossRef]
91. David, L.M.; de Carvalho, R.F. *Bacias de Retenção Para Controlo de Cheias: Reflexão Sobre Métodos de Dimensionamento. Encontro Nacional de Saneamento Básico*; UBI: Beira Interior, Portugal, 2008.
92. Beck, H.E.; Bruijnzeel, L.A.; van Dijk, A.I.J.M.; McVicar, T.R.; Scatena, F.N.; Schellekens, J. The Impact of Forest Regeneration on Streamflow in 12 Mesoscale Humid Tropical Catchments. *Hydrol. Earth Syst. Sci.* **2013**, *17*, 2613–2635. [CrossRef]
93. SNIRH > Dados de Base. Available online: https://snirh.apambiente.pt/index.php?idMain=2&idItem=1&objCover=920123704&objSite=920685506 (accessed on 6 March 2023).
94. Chow, V.-T. *Handbook of Applied Hydrology*; McGraw-Hill: New York, NY, USA, 1964.
95. Gonçalves, J.A.V. Caracterização do Coeficiente de Rugosidade e Seu Efeito no Escoamento em Canais Naturais: Simulação e Modelação (à Escala) no Laboratório de Hidráulica: Aplicação às Ribeiras do Funchal. Master's Thesis, Universidade da Madeira, Funchal, Madeira, Portugal, 2017.
96. Plano de Gestão de Riscos de Inundação Da RAM-PGRI-RA–Google Drive. Available online: https://drive.google.com/drive/folders/0BxPHHom7Ioe6bUQybkdoY2RvSVE?resourcekey=0-YYBZnl-ByzCMyDd6INwQUg (accessed on 6 March 2023).
97. Castanho, R.A. Evolución del Procedimiento de Planeamiento Urbano en la Península Ibérica y sus Huellas en el Paisaje Urbano. Retos de futuro. *Rev. Científica Monfragüe Desarro Resiliente Extremadura Spain* **2017**, *8*.
98. Fadigas, L. *Urbanismo e Território—As Políticas Públicas | Edições Sílabo*; Edições Sílabo: Lisbon, Portugal, 2015.
99. Loures, L. Planning and Design in Postindustrial Land Transformation: East Bank Arade River, Lagoa-Case Study. Ph.D. Thesis, University of Algarve, Faro, Portugal, 2011.
100. Alexandre Castanho, R.; Lousada, S.; Manuel Naranjo Gómez, J.; Escórcio, P.; Cabezas, J.; Fernández-Pozo, L.; Loures, L. Dynamics of the Land Use Changes and the Associated Barriers and Opportunities for Sustainable Development on Peripheral and Insular Territories: The Madeira Island (Portugal). In *Land Use-Assessing the Past, Envisioning the Future*; Carlos Loures, L., Ed.; IntechOpen: Rijeka, Croatia, 2019; ISBN 978-1-78985-703-0.
101. Yu, B.Y.; Wu, P.; Sui, J.; Ni, J.; Whitcombe, T. Variation of Runoff and Sediment Transport in the Huai River—A Case Study. *J. Environ. Inform.* **2020**, *35*, 138–147. [CrossRef]
102. Shrestha, N.K.; Wang, J. Water Quality Management of a Cold Climate Region Watershed in Changing Climate. *J. Environ. Inform.* **2019**, *35*, 56–80. [CrossRef]
103. Li, Z.; Li, J.J.; Shi, X.P. A Two-Stage Multisite and Multivariate Weather Generator. *J. Environ. Inform.* **2019**, *35*, 148–159. [CrossRef]
104. Vargues, P.; Loures, L. Using Geographic Information Systems in Visual and Aesthetic Analysis: The Case Study of a Golf Course in Algarve. *WSEAS Trans. Environ. Dev.* **2008**, *4*, 774–783.
105. Nunes, J.R.; Ramos-Miras, J.; Lopez-Piñeiro, A.; Loures, L.; Gil, C.; Coelho, J.; Loures, A. Concentrations of Available Heavy Metals in Mediterranean Agricultural Soils and Their Relation with Some Soil Selected Properties: A Case Study in Typical Mediterranean Soils. *Sustainability* **2014**, *6*, 9124–9138. [CrossRef]